

Mechanical Characterization of Microelectrodes: Used for Auditory Cortical Prostheses

Ariba Chowdhury¹, Katie L. Harrigan², Devang Ghandi³, Ronnie Das³, and Patrick J. Rousche³

¹ *Department of Biomedical and Chemical Engineering, Syracuse University, Syracuse, NY*

² *Department of Applied Biology and Biomedical Engineering, Rose-Hulman Institute of Technology, Terre Haute, IN*

³ *Neural Eng. Device and Development Laboratory and Neural Eng. Application Laboratory, University of Illinois at Chicago, Chicago, IL*

I. INTRODUCTION

Microelectrodes implanted in human cortical tissue are neuroprosthetic devices known as cortical neural prosthetics (CNPs), systems designed to stimulate areas of the brain [7]. This type of Brain Machine Interface (BMI) has the ability to record and send signals within the cortical membrane to enhance and replace natural movements in individuals suffering from neurological defects [5]. The usage of electrodes allows bypassing biological pathways and the CNS to establish a direct communication between computer systems and the brain [9]. In the case of our research, the advancement and implications are geared towards the implantation of microelectrodes into the auditory cortex. However, such technological application may advance to be implanted into other cortical regions.

Internal electrodes behave based on the electrode-electrolyte interface created upon implantation, such an interface is maintained by extracellular fluid (cerebrospinal fluid within the dura matter) [9, 1]. However, several studies of CNPs indicate that the effectiveness (the ability to properly transmit and record signals) of electrodes is time dependent [9, 8]. The short life span is caused by several factors within the interface. Most fabrication of electrodes has been of metal based which were insulated by a biocompatible polymer. The polymer prevents the biological tissue to carry out its defensive mechanisms of encapsulation of the electrode since the material does not signal or cause any harm to the tissue itself [5]. However, the continuous exposure to blood vessels, cellular components, and immune system fluids upon insertion into cortical tissue denatures the electrode's efficiency [9]. Also, if the insertion of an electrode causes damage of

tissue or neurons, proliferation of astrocytes leads to encapsulation of the electrode [9]. Thus, to minimize the occurrence of such damage and motion artifacts, flexible electrodes have been synthesized for replacement to easily conform to tissue movement and behavior [9].

Microelectrodes must be miniscule in size, flexible to become mechanically invisible, strong to penetrate through the cortical membrane without causing damage and remain mechanically stable upon completion of implantation [9]. Mechanical disruption of the electrode-tissue interface may cause adverse reactions to both electrode performance and/or biological tissue. The advancement of such CNPs depends on the understanding of the effects and prevention of such disruptions.

Previous research has indicated characteristics of rat cerebral cortex upon insertion of single-tine microelectrodes [4]. However, there have been no studies indicating the change in the mechanical behavior of the implanted electrode due to low frequency bodily movement.

To consider this aim, studies of the penetration of polyimide insulated stainless steel single shaft microelectrodes (125 μm) into human and rat cadaver brain tissue have been done, which revealed data illustrating the kinds of mechanical forces at work upon this junction. Force relaxation traces were obtained across human cadaver primary auditory cortex, Heschl's gyrus (HG) and rat cadaver auditory cortex located in the posterolateral neocortex [1, 4]. The various brain tissues were actuated at 3 Hz with the electrode inserted into the HG to observe the change of forces. Forces experienced by the electrode may help to indicate the tissue properties evident in the cortex as well as the

effective limitations of the microelectrode. Upon establishment of an optimal protocol of measurements, it will be applied to the flexible polyimide-based cortical microelectrode arrays currently being fabricated in the Rousche lab.

II. METHODS AND MATERIALS

A. Tissue Sample

Formalin fixed (10% formaldehyde) human brain (n=8) (FHB) was obtained from Dr. Robert Wollman from the University of Chicago. Formalin fixed (FRB) (10% formaldehyde) and non formalin fixed (NRB) rat brain were obtained from Terry Chiganos of University of Illinois at Chicago.

B. Mechanical Set Up

A 500 mN thin film strain gage load cell (S100, SMD Sensors) was mounted on a three-dimensional micromanipulator (fig. 1A). A $\pm 10V$ DC power supply was utilized as an excitation voltage. Shown in figure 2, 125 μm polyimide insulated stainless steel single shaft (Plastics 1) microelectrodes were attached to the load cell and penetrated cadaver cortical tissue. An instrumentation operational amplifier (AD620, Analog Devices) was utilized to amplify and filter the signal (fig. 1B), while a 12-bit data acquisition system (Model #158UP, Windaq) was used to acquire the signal at 240 Hz. A DC electric motor (Radio Shack) was purchased and powered by another $\pm 10V$ DC power supply to actuate the tissue at 1-3 Hz. Calibration and analysis was performed on the load cell.

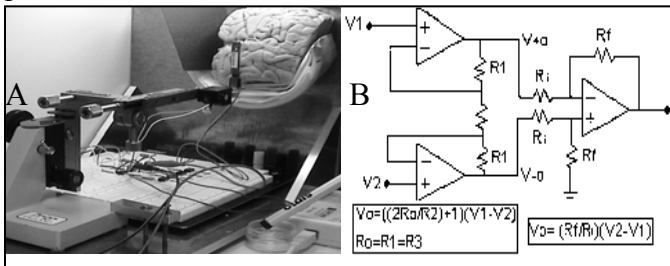


Figure 1. Experimental setup. A) Picture of the experimental setup including the FHB tissue, electrode mounted on a load cell, B) A schematic of the operational amplifier AD620 used to amplify and filter the signal with a gain of 1000.

Figure 2. Cross sectional diagram of the electrode viewed perpendicular to the electrode surface. The diameter of the

coated or uncoated metal wire is exaggerated in this representation for ease of viewing.

C. Experimentation: Human and Rat Brain Tissue

Tissue	trial	Insertion (mm)	Increment (mm)	Rows (mm)	Separation (mm)	Actuation (Hz)
Formalin Human Brain	1	3.5	10.0	2.0	5.0	3.0
	2	1.0	5.0	2.0	5.0	3.0
	3	1.0	2.0	3.0	2.0	3.0
Formalin Rat Brain	A 1	1.0	2.0	2.0	2.0	3.0
	A2	1.0	2.0	3.0	2.0	3.0
	B 1	1.0	2.0	3.0	2.0	3.0
Non	A 1	1.0	2.0	2.0	4.0	3.0
Formalin Rat Brain	B1	3.5	1.0	3.0	1.0	3.0, 7.0, >7.0
Brain	C1	1.0	1.0	2.0	1.0	3.0, 7.0, >7.0

Experimentation pertaining to Non Formalin Fixed Rat Brain varied for samples B1 and C1. For all other samples of cortical tissue, the protocol was the same, where the tissue sample was held within a chamber and the electrode was maneuvered (by the micromanipulator) into the tissue.

However, for B1 and C1, the rat brain tissues were exposed while they were in situ. Upon approval of procedures with the UIC Animal Care Guidelines, the rats were placed in an airtight chamber and CO_2 was used for euthanization. Data were collected from two Sprague-Dawley rats. An incision was made down the midline of the cranium and the underline fascia was removed to expose the skull. Two craniectomies were performed bilaterally over the intended regions of implantation (6- 8 mm lateral and 4-5 mm caudal relative to the top surface of the brain). Subsequently, the dura was removed to expose the sub arachnoid surface. The bodies were positioned into the same chamber with their cortical tissue exposed for preparation of electrode insertion by the micromanipulator.

E. Data Analysis

The 12-bit data acquisition system (Model #158UP, Windaq) was used to acquire the signal at 240 Hz. The data was analyzed using software custom-written in Matlab (Matlab 7, Mathworks, Inc.) to reveal forces experienced by the electrode. The curves pertaining to stress relaxation were analyzed by a modified fitting program in Matlab. The fitting equation was based on viscoelastic

models of mechanical systems with applied displacement (x), measured offset (A), measured scaling factor (B), fitted time- constant (τ), and fitted constant phase element (α).

$$F = x (A + B e^{-t^{\alpha}/\tau}) \quad (1)$$

III. RESULTS

A. Calibration

Initial calibration consisted of an analysis of load cell drift and the calculation of the calibration conversion factor (CCF). The load cell took 25-30 min to achieve an initial steady-state response and the CCF=2.959 mg/mV ($R^2=0.997$). The load cell maintained a systematic error of 9.4% throughout experimentation.

B. Force Measurement: FHB

A sample of a typical force measurement trace is shown in Fig. 3A. According to Fig. 3, baseline force pre- and post-insertion resulted in a negligible measurement. In figures 4 and 5, the values of the insertion forces, steady state forces, and retraction forces are 18.181 mN, 7.374 mN, and 7.183 mN, respectively. The insertion force required to penetrate through FHB cortical tissue was greater than the steady state forces established within the cortical membrane of HG of FHB by a factor of 3.

C. Force Measurement: FRB

A sample of a typical force measurement trace for FRB is shown in Fig. 3B. According to Fig. 3, baseline force pre- and post-insertion resulted in a negligible measurement. In figures 4 and 5, the values of the insertion forces, steady state forces, and retraction forces are 39.453 mN, 13.308 mN, and 12.245 mN, respectively. The insertion force required to penetrate through FRB cortical tissue was greater than the steady state forces established within the cortical membrane of FHB by a factor of 3.

D. Force Measurement: NRB

A sample of a typical force measurement trace for NRB is shown in Fig. 3A. According to Fig. 3, baseline force pre- and post-insertion resulted in a negligible measurement. In figures 4 and 5, the values of the insertion forces, steady state forces, and retraction forces are 8.584 mN, 2.825 mN, and 1.454 mN, respectively. The insertion force required to penetrate through NRB cortical tissue was greater than the steady state forces established within the cortical membrane of NRB by a factor of 3.

Force Measurement Traces of Cortical Tissue

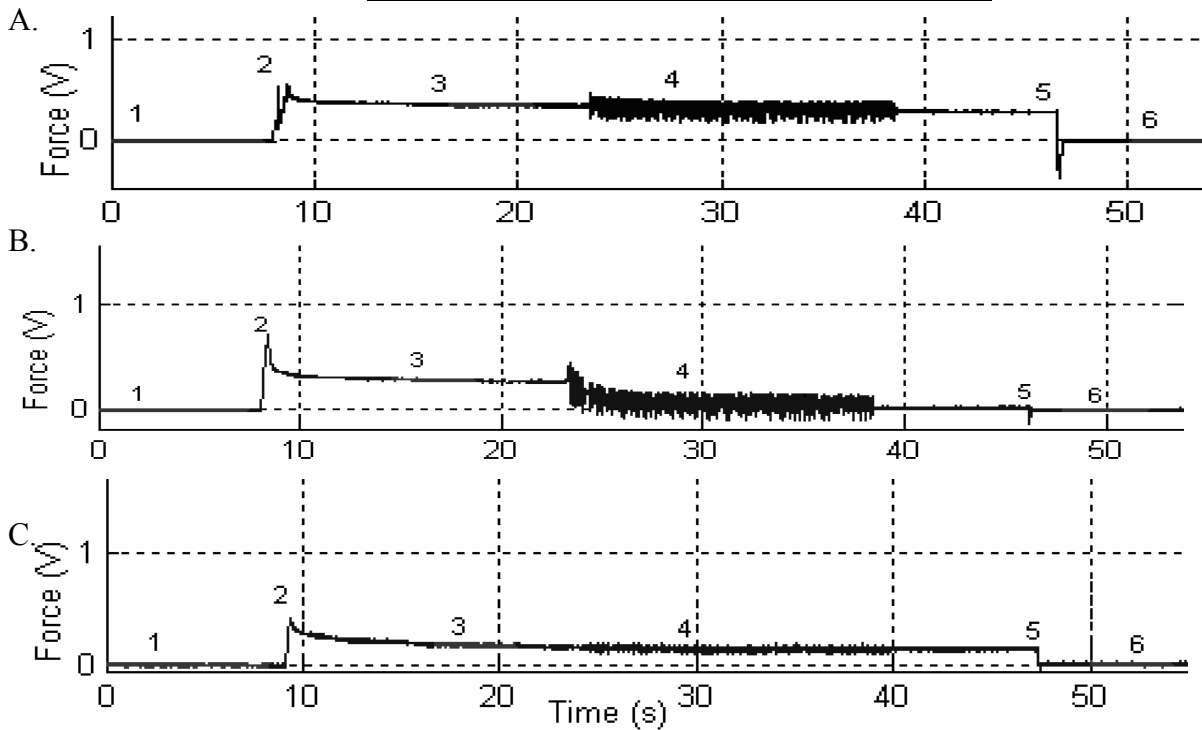


Figure 3. Force Data Evaluation with parameters numbered as: 1: initial baseline, 2: peak upon insertion, 3: steady state, 4: actuation at 3 Hz., 5: neg. peak upon retraction, and 6: final baseline. Polyimide insulated stainless steel single shaft electrode insertion and actuation applied in A) FHB, B) FRB, and C) NRB.

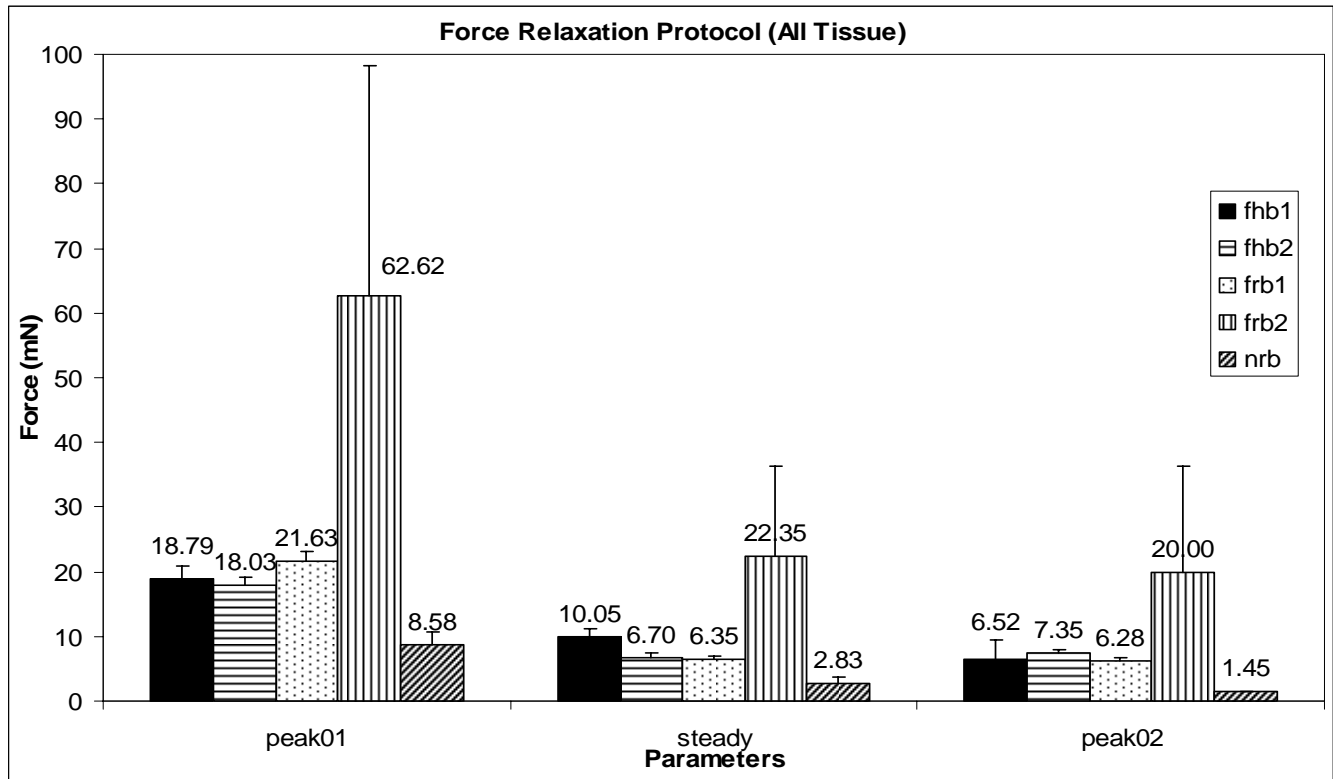


Figure 4. Force Relaxation in all Samples. Parameters highlighted are peak01 (insertion forces), steady (steady state forces), and peak02 (retraction forces). The graph is based on an average taken from the set samples converted from Voltage (volts) (output of the load cell measurements) into Force (mN) by conversion factor established from calibration of 2.959 mg/mV.

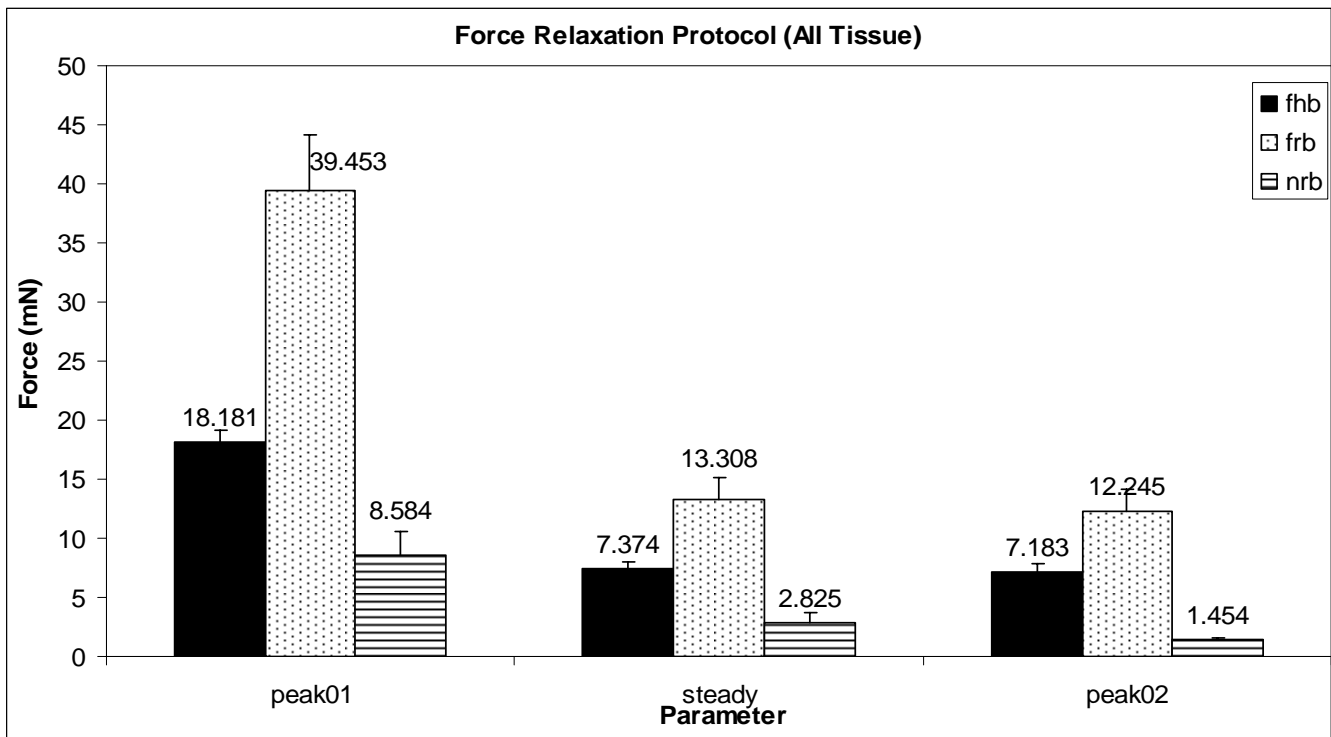


Figure 5. Force Relaxation in Brain Tissues. Parameters highlighted are peak 01 (insertion forces), steady (steady state forces), and peak 02 (retraction forces). The graph is based on an average taken from the set samples converted from Voltage (volts) (output of the load cell measurements) into Force (mN) by conversion factor established from calibration of 2.959 mg/mV.

E. Stress Relaxation Curve Fitting

Stress Relaxation is the viscoelastic decaying behavior which initiates at the insertion force peak as the material conforms to the electrode. Fitting Analysis was performed on the data revealing stress relaxation based on the derived equation (1). The fractional exponent (α) pertains to the constant phase element of viscoelastic property of the cortical tissue. The constant phase element pertains to the fractional order linear model, where the linear dashpot (fig. 6A) is replaced by a fractional component (fig. 6B) [2]. A fractional component behaves partly as a spring and a dashpot representing elastic and viscous properties, respectively. If the model consisted of only a dashpot (viscous module), the decay would be exponential ($\alpha = 1$). If the model consisted of only a spring (elastic module), no decay would be observed ($\alpha = 0$) [2].

In the case of the Fractional Order Linear Model ($\alpha = 1$), there is a time dependent exponential decay representing a viscoelastic property where the decay never reaches zero value. Based on the fitting analysis, the fitted functions showed to be similar to the behavior of the fractional order linear model with optimal r-

squared values ($\approx .98$). In figure 8m typical stress relaxation curves and their fit is shown per tissue. The average fractional exponent (α) is $0.4 \pm .12$ for FHB, $0.5 \pm .27$ for FRB, and $0.6 \pm .16$ for NRB (fig. 8)

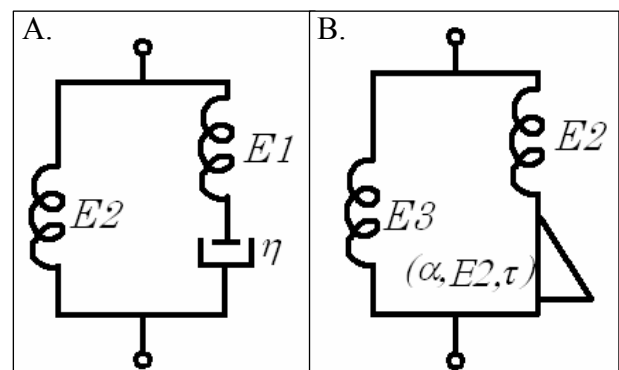


Figure 6. Models of Transient Response to a Unit Step Input of Stress. A) Linear Model ($\alpha = 1$), B) Fractional Order Linear Model ($0 < \alpha < 1$), where $E1$, $E2$ and $E3$ are springs: elastic modules; η is a dashpot: viscous module, and the fractional component: (α , $E2$, τ) a time dependent viscous module.

Stress Relaxation Trace Fits of Brain Tissue

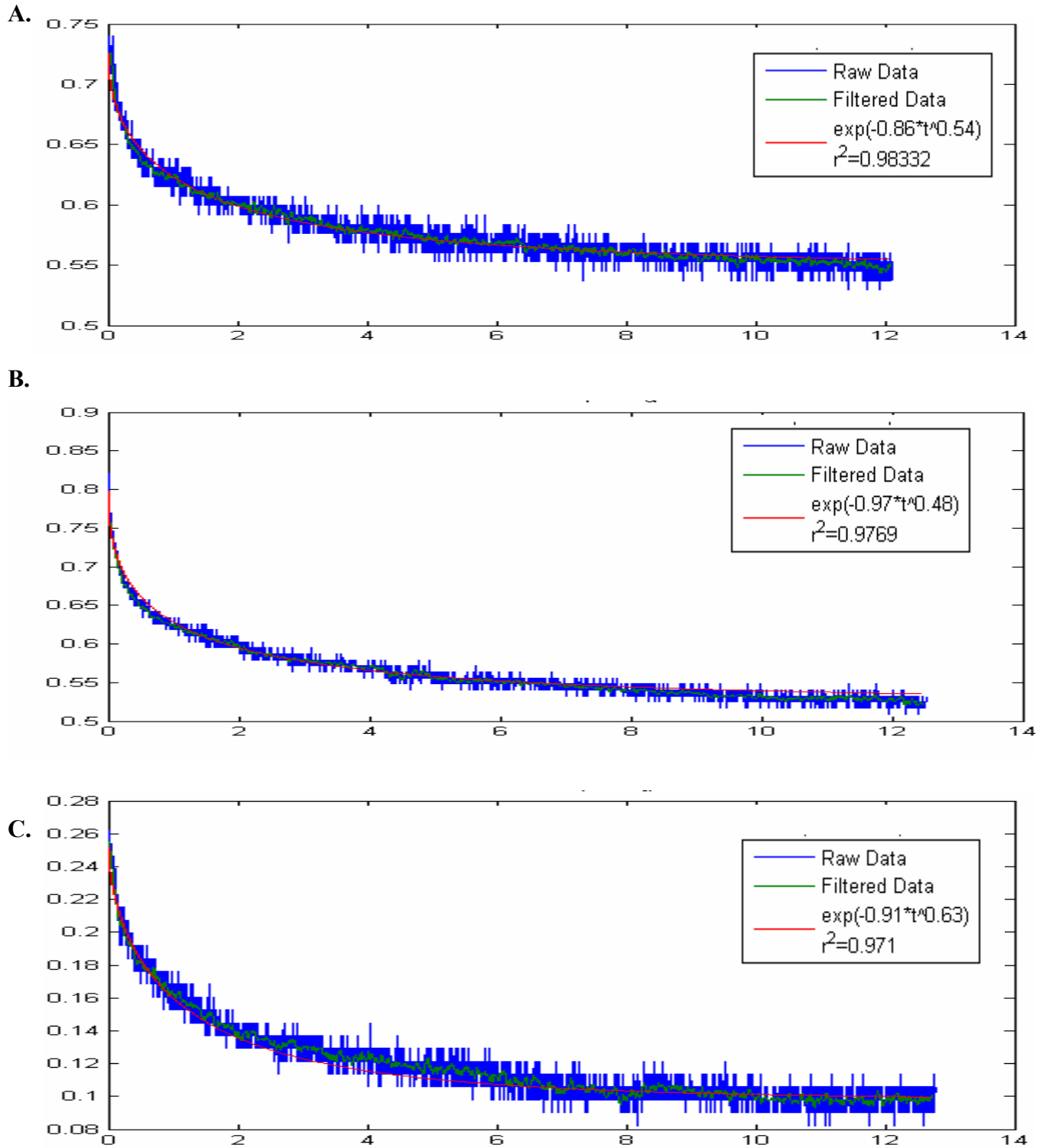


Figure 8 a-c. Stress Relaxation Fits of Cortical Tissues. Data Fit Analysis was performed on the filtered data (sectional averages to filter out noise) based on equation (1). A) FHB, B)FRB and C) NRB.

IV. CONCLUSION

Based upon these initial results shown in figures 4 and 5, we can conclude that polyimide insulated stainless steel single shaft microelectrodes must be stiff enough to withstand penetration forces as high as 18.181 mN and plastic forces of 7.183 mN if inserted in FHB, 39.453 mN and 12.245 mN if inserted in FRB and 8.584 mN and 2.825 mN if inserted in NRB. In following experimentation with such brain tissue and other electrodes, these resulting force measurements can be utilized to establish steady state upon insertion of electrode.

The steady state force is the force that the electrode is experiencing while it is within the tissue. If implanted, the electrode must be able to effectively transmit and record signals while constantly receiving such a force onto its structure. This factor should be considered when fabricating an electrode for the purpose to be implanted in intended tissue.

The force measurements at different parameters allow validation of certain properties of cortical tissue. The forces required to insert the electrode into the tissues were always larger than the steady state forces by a factor of 2-3. This indicates that force is being applied from the surface which was opposing the force experienced during insertion. This exertion of force from the tissue surface is evident of a resistive property of the cortical tissue, indicating a viscoelastic surface which is directly related to the thickness of the tissue of a region. But, the force from the tissue acting on the electrode establishes a point in which the penetration occurs, electrode force is higher than tissue force (the insertion force peak), indicates a force dependent relationship established within this junction. Thus, the insertion occurs due to the elastic property of the tissue responding to the load application. Upon more experimentation, and based on the models theorized by Maxwell and Voigt, a non-linear viscoelastic model can be established pertaining to the cortical tissue of FHB, FRB and NRB [3]. Such a model can help to understand the force behavior changes related to electrode insertion and establishment of steady state following insertion.

Stress Relaxation, the viscoelastic decaying behavior (initiates at the insertion force peak) occurs while the brain tissue conforms to the electrode. Fitting Analysis was performed on the data, based on the function (1) from the Fractional Order Linear Model ($\alpha = 1$). In each tissue, a similar time dependent exponential decay of the fitted functions were observed, representing the viscoelastic property. The fitted functions showed to be similar to the behavior of the fractional order linear model with optimal r-squared values ($\approx .98$). Even though the fractional exponent varies within a tissue, this variation is seen throughout all the tissues. So the viscosity of the tissues is not constant within itself, but all tissues do reveal the same stress relaxing property, similar to the fractional order linear model.

The retraction force also indicates properties of the cortical tissue. In each tissue, during removal of the electrode, force was exerted from the tissue onto the electrode, indicating tensile property of the tissue. If an n amount of force is supplied to penetrate the tissue, one would expect removal to occur without any force acted on the electrode because the penetration force has already been reached by the electrode. However the opposite is observed, indicating that the tissue clings onto the polyimide insulated shaft and thus the retraction force is directly related to the force the tissue uses to keep the electrode within itself (steady state forces). Its limitation is the retraction force established.

Forces measured for the NRB is significantly lower than the FRB tissue, indicating that formalin fixed cortical tissue are stiffer than natural cortical tissue. Thus, upon more experimentation, a relationship between natural and formalin tissue can be concluded and utilized to hypothesize the behavior of real human cortical tissue in comparison to formalin fixed human cortical tissue. Future experiments will be done to continue actuation on tissues to observe the difference and affect of actuation (3 Hz, 7 Hz and >7 Hz) on the cortical tissue- electrode interface.

ACKNOWLEDGEMENTS

I would like to thank the Laboratory of NEDDL and NEAL for support and guidance throughout this research project. Also, I would like to acknowledge the National Science Foundation and the Research Experience for Undergraduates Program at University of Illinois at Chicago for support and funding of the work (NSF EEC-0453432 Grant, Novel Materials and Processing in Chemical and Biomedical Engineering).

[1] Bear M.F., Connors B.W., and Paradiso M.A. Neuroscience: Exploring the Brain, Second Edition. Maryland: Lippincott Williams & Wilkins, 2001.

[2] Bourne, John R. Critical Reviews in Biomedical Engineering. New York: Begell House, Inc., 2004.

[3] Fung, Y.C. First Course in Continuum Mechanics, Third Edition. New Jersey: Prentice Hall, 1994.

[4] Jensen W., Hofmann U.G., and Yoshida K. "Assessment of Subdural Insertion Force of Single-Tine Microelectrodes in Rat Cerebral Cortex." 25th Annual Int. Conference of the IEEE- Engineering in Medicine & Biology Society. (2003) 2168-2171.

[5] Kolb, B and Tees, R. C. The Cerebral Cortex of the Rat. Massachusetts: The MIT Press, 1990.

[6] Lakshmi S. Gandhi D., Das R., and Rousche P.J. "Analysis of *In- vitro* Neurite Extension for Neurotrophic Electrode Design." Proceedings of the 2nd International IEEE EMBS Conference on Neural Engineering. (2005):v-vii.

[7] Maynard E.M., Fernandez E., and Normann R.A. "A technique to prevent dural adhesions to chronically implanted microelectrode arrays." *Journal of Neuroscience Methods*. 97(2000): 93-101.

[8] Schwartz, Andrew B. "Cortical Neural Prosthetics." *Annu. Rev. Neurosci.* 27 (2004): 487-507.

[9] Webster, J.G. Medical Instrumentation: Application and Design, Third Edition. Canada: John Wiley & Sons, Inc., 1998.

REFERENCES